The Modification of Lanthanum-Exchanged Montmorillonite with Anionic Surfactants to Enhance the Thermal Stability of Polyvinyl Chloride

Haijiao Wang, Heyun Wang, Kai Chen, Yanmei Song, Zhong Wei, Mei Xue

School of Chemistry and Chemical Engineering/Key Laboratory for Green Processing of Chemical Engineering of Xinjiang Bingtuan, Shihezi University, Shihezi 832000, China
Correspondence to: Z. Wei (E-mail: steven_weiz@sina.com)

ABSTRACT: A series of thermally stable lanthanum organic montmorillonites (La-OMMTs) were successfully prepared by modifying Na-MMT with anionic surfactants and lanthanum chloride. Fourier transform infrared spectroscopy and X-ray diffraction indicated that the anionic surfactants resided in the interlayer spaces and expanded the MMT basal spacing from 1.23 nm to 3.3 nm. Thermogravimetric and differential thermal analysis (TG/DTA) results showed that the intercalation of sodium dodecyl sulfonate into the lanthanum organic MMT resulted in its excellent thermal stability. The use of the La-OMMT samples in polyvinyl chloride (PVC) resins was tested, and the TG/DTG results revealed that the three La-OMMTs could significantly enhance the thermal stability of PVC. The modified La-OMMT with the highest thermal stability is expected to be useful in polymer/layered silicate nanocomposites. © 2014 Wiley Periodicals, Inc. J. Appl. Polym. Sci. **2015**, *132*, 41535.

INTRODUCTION

Montmorillonite (MMT) is a layered-type silicate that belongs to the 2 : 1 phyllosilicate structural family. For its large surface area-to-volume ratio, nanosized layered structure, natural abundance, and relatively low cost, MMT has received attention and is desirable for use in nanomaterials and applications.[1–3] Nanocomposites are a combination of two or more phases containing different compositions or structures, where at least one of the phases is in the nanoscale regime. However, the properties of nanocomposites are greatly influenced by the degree of mixing between the organic and inorganic components, the excellent dispersion of MMT is believed to play an important role with the nanocomposite properties.[4] The hydrophilic nature of MMT layer surfaces impeded their homogeneous dispersion in high hydrophobic polymer matrix,[5] resulting in poor interaction forces between the organic and inorganic components and leading to the agglomeration of nanofillers during processing and deterioration of material properties.[6] Therefore, the modification of MMT with organic compounds is paramount for preparing nanocomposites.
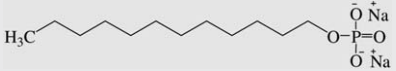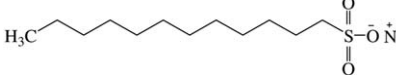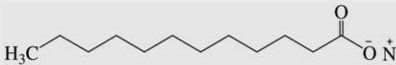
OMMT, which is from MMT organic modification, has been extensively used to prepare the polymer/OMMT nanocomposites.[7–9] Via the modification process, not only can the surface properties of MMT be changed from hydrophilic to hydrophobic, but also the basal spacing of the MMT layers can be greatly increased to achieve nanoscale dispersion.[10] Compared to conventional polymer composites containing traditional fillers, OMMT greatly enhances the mechanical and thermal properties of the polymer, decreases its gas permeability, and expands its potential for application in the aviation, biomedical, and other polymer industries.[11] It is commonly accepted that the addition of a small amount of OMMT ($\leq$10 wt %) can produce a significant improvement in the material properties.[12,13]

In general, OMMT can be prepared with cationic, anionic, and nonionic surfactants. Up to now, most researchers focused on MMT modified with cationic surfactants because they can be easily intercalated into the MMT interlayer space by simple cation exchange.[14,15] However, many reports found that cationic surfactants are thermal instability and could catalyze the degradation of polymer matrixes.[16–18] For instance, the alkyl ammonium salts decomposed around 170–180°C and are not suitable for high-temperature melt processing techniques. Another method for modifying MMT involves the use of nonionic surfactants, such as polyethylene glycol, alcohols, aldehydes, and ketones.[6,19,20] These modified MMTs are commonly used for biodegradation polymers and the remediation of contaminated soils.

Organic modification of MMT with highly thermally stable anionic surfactants has received considerable attention these years. The anionic surfactants could be easily intercalated in MMT by

Table I. Types of Organoclay Samples Produced and Structures of the Intercalating Agents Used

Sample	Anionic surfactant	Structure of the anionic surfactant
La-OMMT-SMDP	Sodium monododecyl phosphate (SMDP) 310.28 g mol^{-1}	
La-OMMT-SDS	Sodium dodecyl sulfonate (SDS) 272.38 g mol^{-1}	
La-OMMT-SDD	Sodium dodecanoate (SDD) 222.30 g mol^{-1}	

ion-dipole attraction with the exchangeable cations located in the gallery of MMT, and the attraction between high valence cations with anionic surfactant was stronger than that of low valence cations.[21] Besides, Liang and Wang found that the anionic surfactants could form precipitate with cations.[22] Chen et al. demonstrated that the dispersion, swelling, and thixotropy properties of MMT modified with anionic surfactants were superior to those of modified with hexadecyltrimethylammonium bromide.[23] Feng et al. reported the preparation of both exfoliated and intercalated OMMT by a precipitation–adsorption process and discussed the mechanism of this method.[24]

Polyvinyl chloride (PVC) is a kind of widely used chlorine-containing thermoplastic. The dehydrochlorination temperature of PVC is around 120°C and the processing temperature is about 170°C. As a result, the application of PVC is limited by its thermal stability significantly. During the preparation of PVC and its nanocomposites, the properties of surfactants which used to prepare OMMT has great influences on the thermal stability of nanocomposites, especially for the alkyl ammonium salts cationic surfactants. The degradation of alkyl ammonium salts could accelerate the dehydrochlorination rate of PVC significantly.[25]

In the recent years, different kinds of thermal stabilizers are incorporated into PVC applications in order to restrain the degradation of the polymer. A great number of studies have demonstrated that organic acid lanthanum salts have an excellent thermal stabilization effect on PVC.[26–32] Besides, Lanthanum ions and anionic surfactant could form strong interaction of coordination and precipitation, which could be more favorable of anionic surfactant entering into the MMT interlayer and forming more stable structure of lanthanum organic montmorillonites (La-OMMT). To the best of our knowledge, research about preparing La-OMMT by reacting La-MMT with anionic surfactants and their applications on thermal stability of PVC have not been reported so far.

In this article, different types of La-OMMT with high thermal stability were prepared by modifying Na-MMT with lanthanum chloride and three anionic surfactants, through a precipitation–adsorption method. The La-OMMTs were characterized with X-ray diffraction (XRD), Fourier transform infrared (FTIR) spectroscopy, thermogravimetric analysis (TGA) and inductively coupled plasma-atomic emission spectrometry (ICP-OES). The influences of the La-OMMTs to the thermal stability of PVC and its nanocomposites were also studied by various techniques.

EXPERIMENTAL

Materials

Sodium MMT (Nanocor) was supplied by Beijing East-West Technology Ltd., which provided a list of the Na-MMT properties. The purchased Na-MMT sample had a basal spacing of 1.23 mm and cation exchange capacity (CEC) of 143 meq/100 g. The anionic surfactants including sodium monododecyl phosphate (SMDP), sodium dodecyl sulfonate (SDS), and sodium dodecanoate (SDD) were obtained from Aladdin and used without further purification. The organic La-MMT was modified by SMDP, SDS, or SDD and denoted as La-OMMT-SMDP, La-OMMT-SDS, and La-OMMT-SDD, respectively. LaCl$_3$•6H$_2$O was obtained from Changsha Shengyang Chemical Material Co., Ltd. (China). The PVC resin (SG-5 type, suspension grade) was kindly provided by Xinjiang Tianye Chemical Plant (Xinjiang, China). All materials were used as received without further purification. Doubly distilled water was used in the experiments. The three anionic surfactants used in this study are listed in Table I.

Preparation of Organo-Montmorillonite

La-MMT was prepared by a cationic-exchange reaction. Pristine Na-MMT was suspended in distilled water (1 g of powdered clay in 30 mL) at room temperature, and the dispersion was stirred vigorously for 24 h to obtain fully swollen Na-MMT. The pH of the Na-MMT suspension was then adjusted to ∼5 with hydrochloric acid. The LaCl$_3$•6H$_2$O solution was added dropwise to the Na-MMT suspension under continuous, vigorous stirring at 60°C for 2 h. The total amount of solution added was equivalent to three times the CEC of Na-MMT. La-OMMT was prepared by exploiting the ion-dipole attractions between La-MMT and the anionic surfactants. The surfactants were dissolved in distilled water. The amount of surfactant added was equivalent to two times the CEC of Na-MMT. Then, the pH of the La-MMT suspension was adjusted to ∼8, and the surfactant solution was slowly added. After the reaction mixture was vigorously stirred at 60°C for a given reaction time, the products were obtained by centrifugation and washed repeatedly with hot deionized water and 50% ethanol to remove the chloride ions and excess surfactant. The final products were vacuum dried at 60°C and pulverized to pass through a 200-mesh sieve. Consequently, three different La-OMMT samples were obtained.

Preparation of La-OMMT/PVC Nanocomposites

To test the potential use of the La-OMMT samples in PVC resin, various La-OMMT/PVC nanocomposites were prepared
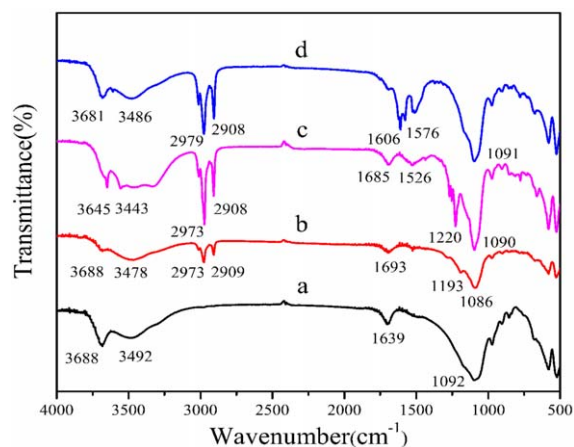
Figure 1. FTIR spectra of (a) Na-MMT, (b) La-OMMT$_{SMDP}$, (c) La-OMMT$_{SDS}$, (d) La-OMMT$_{SDD}$. [Color figure can be viewed in the online issue, which is available at wileyonlinelibrary.com.]

via a solution blending method. PVC and 3 wt % La-OMMT were dissolved in THF by sonication at room temperature. Then, the mixed solutions were cast on Petri dishes, and the solvent was removed by evaporation in a vacuum oven at 80°C for 48 h. Finally, three different La-OMMT/PVC films were produced and tested with TGA.

Characterization Methods

Fourier Transform Infrared Spectroscopy. The FTIR spectra were collected in the range of 4000–500 cm^{-1} at a resolution of 4 cm^{-1} using a Nicolet 360 FTIR spectrometer. The different samples were mixed and ground with KBr powder, pressed into tablets, and analyzed. *X-ray diffraction.* The powder XRD patterns were recorded between 1.6° and 10° at a step size of 0.01° using a Bruker D8 Advance diffractometer with Cu K$_\alpha$ radiation (40 kV and 40 mA). Bragg's equation was used to calculate the distances corresponding to the 2θ values of the peaks. TGA was performed on a Netzsch STA 449F3 instrument. Samples of approximately 5–8 mg were heated from 50°C to 750°C at a heating rate of 10°C min^{-1} under a flowing nitrogen atmosphere.

The La(III) content in the organoclay was determined by Inductively Coupled Plasma-Optical Emission Spectrometry (ICP-OES: Thermo Scientific iCAP 6000 Series). A closed-vessel microwave digestion system (CEM-MARS5, American) equipped with fiber optic temperature and pressure sensors were used for sample digestion. Accurately weighed La-OMMT samples (0.1000 g) were transferred to a Teflon digestion vessel avoiding contact with the side of the vessel. Nitric acid (GR, 8 mL) was added, followed by hydrogen peroxide (35%, 2 mL) and hydrofluoric acid (40%, 3 mL) added to the vessel using a graduated pipette. The vessel was sealed and left for about 15 min to ensure complete reaction. The sample was digested in a microwave according to certain heating procedures. After cooling to room temperature, the vessel was unsealed and the inner wall and lid were thoroughly rinsed with 3% HNO$_3$ solution. The solution was filtered through filter paper into a 50-mL volumetric flask. Then, La (III) content was analyzed by ICP-OES. The standard curve was obtained by diluting the standard

solution in different multiples. The solution blank was prepared under the same conditions as in sample preparation but without adding the La-OMMT.

RESULTS AND DISCUSSION

FTIR Spectral Analysis

The FTIR spectra of Na-MMT and the La-OMMTs are shown in Figure 1. The band at 3688 cm^{-1} was assigned to the asymmetric stretching vibration of the structural Al—OH or Si—OH groups of Na-MMT, while the band at 3492 cm^{-1} was due to the —OH stretching of interlayer water. The absorption peaks in the region of 1639 cm^{-1} were attributed to the —OH bending of adsorbed water. The band at 1092 cm^{-1} was due to the Si—O stretching vibration of Na-MMT. Compared to the Na-MMT spectrum, the La-OMMT FTIR spectra exhibited new characteristic bands at 2973 cm^{-1} and 2908 cm^{-1}, which were associated with the C—H stretching vibration of methylene. Additional characteristic bands at 1193 cm^{-1}, 1220 cm^{-1}, and 1606 cm^{-1} were assigned to the P═O groups, S—O stretching vibration of the sulfonate, and symmetric stretching vibrations of the —COO$^-$ groups of the carboxylate ions, respectively.[19] In addition, the band at 3492 cm^{-1} corresponding to the water —OH deformation was observed in the spectra of both the natural Na-MMT and La-OMMTs, but it was slightly shifted toward the lower frequencies in La-OMMTs. These shifts implied that some interlayer water might be removed from the galleries when the long-chain fatty acid anions intercalated into La-MMTs. All these results indicated that three different types of La-OMMTs were prepared successfully.

XRD Analysis

The XRD patterns supplied very useful information on the interlayer spacing of the final intercalated La-OMMTs. The success of the intercalation was mainly verified by measuring the increase in the basal (001) *d*-spacing. Figure 2 shows the XRD patterns of Na-MMT, La-MMT, and La-OMMTs. The typical XRD reflection of Na-MMT related to the basal spacing between the clay platelets appeared at 2θ = 7.21°, which corresponds to a 1.23 nm interlayer spacing. This reflection shifted to 6.02° in
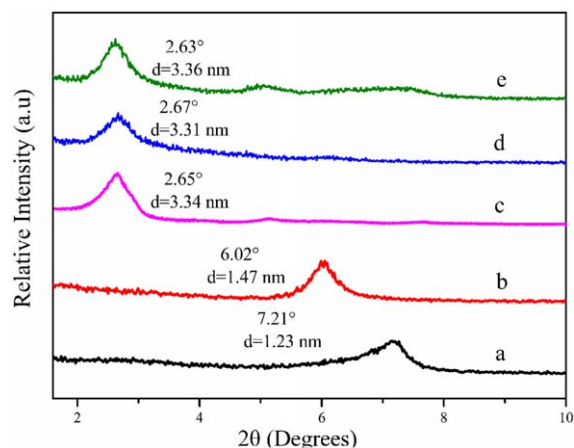
Figure 2. XRD patterns of (a) Na-MMT, (b) La-MMT, (c) La-OMMT$_{SMDP}$, (d) La-OMMT$_{SDS}$, (e) La-OMMT$_{SDD}$. [Color figure can be viewed in the online issue, which is available at wileyonlinelibrary.com.]
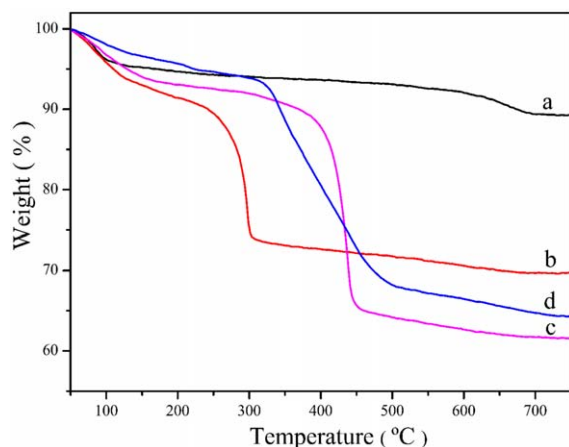
Figure 3. TG curves of (a) Na-MMT, (b) La-OMMT-SMDP, (c) La-OMMT-SDS, (d) La-OMMT-SDD. [Color figure can be viewed in the online issue, which is available at wileyonlinelibrary.com.]
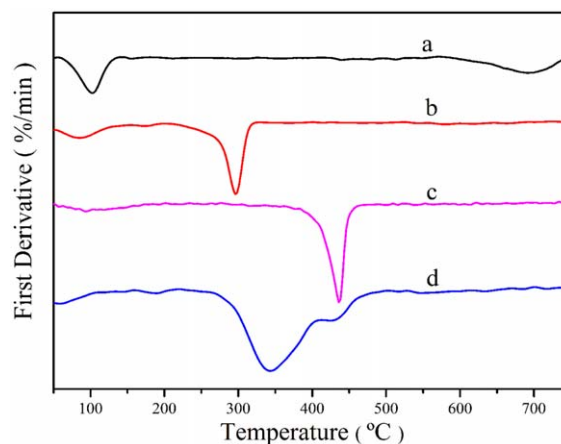

Figure 4. DTG curves of (a) Na-MMT, (b) La-OMMT-SMDP, (c) La-OMMT-SDS, (d) La-OMMT-SDD. [Color figure can be viewed in the online issue, which is available at wileyonlinelibrary.com.]

the La-MMT, meaning an increase in the basal spacing from 1.23 nm to 1.47 nm. After modification with SMDP, SDS, and SDD, this peak shifted to lower angles (2.65°, 2.76° and 2.63°, respectively) corresponding to basal d-spacings of 3.34 nm, 3.31 nm, and 3.36 nm, respectively. The strong, broader reflection peak for the characteristic d-spacing distance shifted to lower angles. The interlayer spacings of La-OMMT-SMDP, La-OMMT-SDS, and La-OMMT-SDD were found to be higher than that of natural Na-MMT. The increase in the modified La-OMMT interlayer spacing was due to the presence of long-chain SMDP, SDS, and SDD in the gallery regions. The following explanation of how the three different types of anionic surfactants entered into La-MMT interlayer spaces might further aid in understanding the basal d-spacing results. Lanthanum ions replaced sodium ions among Na-MMT layers to form La-MMT via ion exchange, making the basal spacing extend to 1.47 nm, for a bigger cationic volume. Then anionic surfactants combined with lanthanum ions with strong interactions of coordination and precipitation and entering the interlayer space as ion pairs with La^{3+} form more stable structure of La-OMMT, which further increase the basal spacing to 3.3 nm. On the other hand, we also found that the basal d-spacing of the La-OMMT-SMDP, La-OMMT-SDS, and La-OMMT-SDD samples were nearly the same, which could be explained by the similar chain length of the three anionic surfactant molecules and their arrangement in the MMT galleries. All these findings indicated that anionic surfactants were intercalated into the La-MMT interlayer spacing and not physically adsorbed on the external surface.
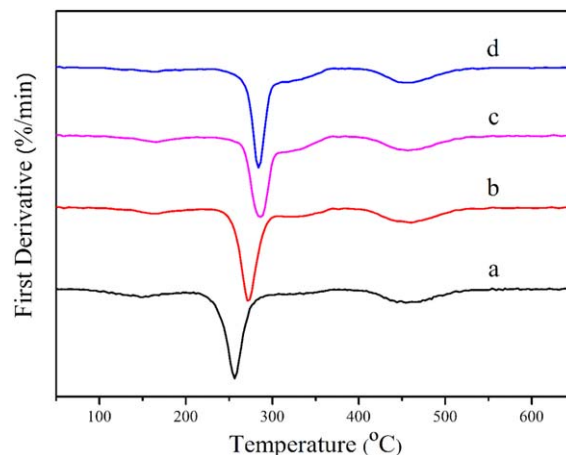
Thermal Gravimetric Analysis

TGA was a useful method for studying the thermal stability of the La-OMMTs and amount of intercalated products. The TG and DTG results of natural Na-MMT and the La-OMMT samples are shown in Figures 3 and 4. For Na-MMT, a mass loss of 5.31% was observed below 200°C and corresponded to the removal of water molecules adsorbed on the surface, which were easier to remove due to their greater mobility. In this low-temperature region, the mass loss percentages of La-OMMT-SMDP, La-OMMT-SDS, and La-OMMT-SDD were 8.58%, 6.95%, and 4.24%, respectively. These losses implied that less free water existed at the external surfaces and the amount of free water depended on the environmental conditions. A comparison of the Na-MMT and La-OMMT TG curves showed that the mass losses of all the modified La-OMMT samples in the temperature range of 200–550°C were much larger than that of Na-MMT. These mass losses were attributed to the evaporation or decomposition of the loaded anionic surfactants, indicating that the MMT surface was converted from hydrophilic to hydrophobic. Table II gives the mass losses of the three different types of La-OMMT samples in the different temperature ranges. The thermal stability of the La-OMMTs should be analyzed at 200–350°C, which is the typical processing temperature of high-melting-point polymers (e.g., PVC, PET) used in the preparation of polymer nanocomposites. It must be noted that the mass loss of La-OMMT-SDS (2.41%) was much smaller than that of La-OMMT-SMDP (18.27%) and La-OMMT-SDD (6.92%),

Table II. Thermal Decomposition Results for the La-OMMT Samples

Sample	T_{onset}, (°C)	Mass loss (%)				Temperature at the maximum decomposition rate (°C)
		T<200 °C	T: 200–350°C	T: 350–550°C	T: 550–750°C	
Na-MMT	72.90	5.31	0.88	1.23	3.27	
La-OMMT-SMDP	283.90	8.58	18.27	1.96	1.46	296.20
La-OMMT-SDS	416.30	6.95	2.41	27.28	1.78	436.60
La-OMMT-SDD	322.50	4.24	6.92	21.59	2.85	341.90
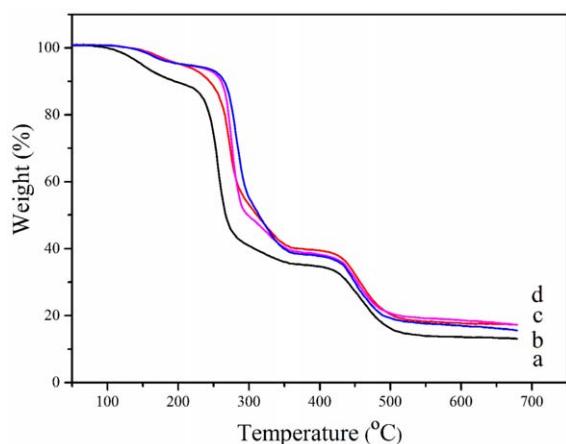
Figure 5. TG curves of (a) PVC, (b) La-OMMT$_{-SMDP}$/PVC, (c) La-OMMT$_{-SDS}$/PVC, (d) La-OMMT$_{-SDD}$/PVC. [Color figure can be viewed in the online issue, which is available at wileyonlinelibrary.com.]

Figure 6. DTG curves of (a) PVC, (b) La-OMMT$_{-SMDP}$/PVC, (c)La-OMMT$_{-SDS}$/PVC, (d) La-OMMT$_{-SDD}$/PVC. [Color figure can be viewed in the online issue, which is available at wileyonlinelibrary.com.]

suggesting that La-OMMT$_{-SDS}$ had higher thermal stability. In addition, the thermal stability of the La-OMMTs in this region is very important for their functioning as polymer nanofillers because the interlayer surfactants begin to decompose in this temperature range. For the La-OMMT$_{-SMDP}$ samples, a large weight loss (18.27%) was observed in the temperature range of 200–350°C. The thermal degradation of La-OMMT$_{-SDS}$ and La-OMMT$_{-SDD}$ occurred between 350 and 550°C and involved both evaporation and complete decomposition of the organic surfactants. Thus, the La-OMMT modified with SDS exhibited an appreciably higher thermal stability than the La-OMMT modified with SMDP or SDD.

The temperature at which the degradation of La-OMMT begins is also essential in determining its thermal stability. The onset decomposition temperatures and temperatures at the maximum decomposition rate from the DTG results are given in Table II. In this article, the onset decomposition temperature was defined as the temperature corresponding to the point of intersection of the two tangents around the main degradation point. This definition was more accurate than the temperature at a 5% mass loss. La-OMMT$_{-SDS}$ had a higher onset decomposition temperature (416.30°C) than La-OMMT$_{-SMDP}$ and La-OMMT$_{-SDD}$ (283.90°C and 322.50°C, respectively). In addition, the temperatures at the maximum decomposition rate determined from the DTG curves were 436.60°C for La-OMMT$_{-SDS}$, 296.20°C for La-OMMT$_{-SMDP}$, and 341.90°C for La-OMMT$_{-SDD}$. These results revealed that the heat resistance of the anionic surfactants intercalated into the La-MMT layers was higher when SDS was used

due to the high thermal stability of the sulfonic acid anion. Moreover, it was clearly shown that the temperature at the maximum decomposition rate was significantly lower for La-OMMT$_{-SMDP}$. It therefore appeared that the thermal stability of La-OMMT$_{-SMDP}$ decreased in the presence of excess surfactants. In summary, La-OMMT$_{-SDS}$ exhibited superior thermal stability compared to La-OMMT$_{-SDD}$ and La-OMMT$_{-SMDP}$.

ICP-OES Analysis

The La contents in the La-OMMT samples were determined by ICP-OES. The amounts of La elements in La-OMMT$_{-SMDP}$, La-OMMT$_{-SDS}$, and La-OMMT$_{-SDD}$ were 8.27%, 8.61%, and 11.99%, respectively. These results indicated that La^{3+} successfully replaced the interlayer spacing cations in Na-MMT via cation exchange. It was also observed that La-OMMT$_{-SDD}$ had a higher amount of La (11.99%) than La-OMMT$_{-SMDP}$ (8.27%) and La-OMMT$_{-SDS}$ (8.61%). Most likely, La^{3+} in La-OMMT$_{-SDD}$ interacted not only with SDD but also with other groups, such as the OH groups at the La-OMMT edges.

Measured Thermal Properties of the La-OMMT/PVC Nanocomposites

Figures 5 and 6 and Table III show the differences in the TG-DTG curves for the PVC and La-OMMT/PVC nanocomposites. The TG-DTG analysis of PVC and the La-OMMT/PVC nanocomposites revealed three stages of decomposition. The first mass loss might be attributed to the evolution of water and solvent retained in the nanocomposites. The second stage of decomposition was related to the degradation of PVC and

Table III. Thermal Decomposition Results for the La-OMMT/PVC Nanocomposites

Sample	2nd stage			3rd stage		
	T_{onset} (°C)	T_{rp2} (°C)	M_{loss} (%)	T_{rp3} (°C)	M_{loss} (%)	Residual at 600°C
PVC	243.32	256.33	54.95	454.91	21.04	13.58
La-OMMT$_{-SMDP}$/PVC	262.01	272.43	57.17	459.53	22.75	14.49
La-OMMT$_{-SDS}$/PVC	273.75	286.44	56.57	456.28	22.33	15.57
La-OMMT$_{-SDD}$/PVC	275.84	284.17	55.66	456.47	22.06	16.04

OMMT. The onset temperature for the thermal decomposition of PVC was found to be 243.32°C. After the addition of La-OMMT, the onset thermal decomposition temperatures of La-OMMT$_{SMDP}$/PVC, La-OMMT$_{SDS}$/PVC, and La-OMMT$_{SDD}$/PVC shifted to 262.01°C, 273.75°C, and 275.84°C, respectively. This phenomenon indicated that La-OMMT could delay the degradation of PVC. It should be mentioned that La-OMMT$_{SDS}$ exhibited superior thermal stability based on the TGA analysis. Consequently, the onset thermal decomposition temperature of La-OMMT$_{SDS}$/PVC was approximately 11°C higher than that of La-OMMT$_{SMDP}$/PVC. Moreover, the La content in La-OMMT$_{SDS}$/PVC and La-OMMT$_{SMDP}$/PVC were similar, indicating that La-OMMT$_{SDS}$ enhanced the thermal stability of PVC to a greater degree. However, the onset thermal decomposition temperature of La-OMMT$_{SDD}$/PVC was the highest, possibly due to the greater amount of La in La-OMMT$_{SDD}$ than in the other La-OMMTs. As mentioned previously, the La rare earth elements have an excellent thermal stabilization effect on PVC. The La content in La-OMMT$_{SDD}$ was 11.99%, which was higher than those in La-OMMT$_{SDS}$ (8.61%) and La-OMMT$_{SMDP}$ (8.27%) based on the ICP-OES results. On the other hand, the onset thermal decomposition temperature of La-OMMT$_{SDD}$/PVC was only approximately 2°C higher than that of La-OMMT$_{SDS}$/PVC. In the third decomposition stage, polyene sequences formed. The La-OMMT$_{SMDP}$/PVC, La-OMMT$_{SDS}$/PVC, and La-OMMT$_{SDD}$/PVC residuals were 14.49%, 15.57%, and 16.04%, respectively, at 600°C and were greater than the pure PVC residual. These results demonstrated that the addition of La-OMMT could promote charring during the degradation process. Comparing with other similar OMMT/PVC nanocomposites about effect of thermal stability, typical cationic surfactants (such as alkyl ammonium salts) modified MMT could catalyze the degradation of PVC[25] and decreased the decomposition temperatures of the OMMT/PVC nanocomposites,[25,33] non-ionic surfactants modified MMT did not reflect obvious influence on the thermal stability of PVC.[34] Jointly using rare earth lanthanum and anionic surfactants, the modified MMT could significantly enhance the thermal stability of polymer, especially in PVC matrix.

CONCLUSIONS

In this study, novel, thermally stable lanthanum organic MMTs were prepared using anionic surfactants. The FTIR analysis indicated that SMDP, SDS, and SDD existed at the surface or in the interlayer spaces of MMT. The XRD results showed that the basal spacings of La-OMMT$_{SMDP}$, La-OMMT$_{SDS}$, and La-OMMT$_{SDD}$ were 3.34 nm, 3.31 nm, and 3.36 nm, respectively. It was demonstrated that the anionic surfactants were intercalated into the La-MMT interlayer spacing and not physically adsorbed on the surface. The TG and DTG results showed that La-OMMT$_{SDS}$ exhibited excellent heat resistance. The onset decomposition temperature of La-OMMT$_{SDS}$ was 132.40°C and 93.80°C higher than those of La-OMMT$_{SMDP}$ and La-OMMT$_{SDD}$, respectively. The ICP-OES results showed that La-OMMT$_{SDD}$ had the highest amount of La (11.99%). Characterization of the La-OMMT/PVC samples indicated that the three La-OMMTs could significantly enhance the thermal stability of

PVC. In summary, these La-OMMTs are promising for use in polymer/layered silicate nanocomposites and related industries.

REFERENCES

1. Leszczyńska, A.; Njuguna, J.; Pielichowski, K.; Banerjee, J. R. *Thermochim. Acta* **2007**, *453*, 75.

2. Valverde, J. L.; Cañizares, P.; Sun Kou, M. R.; Molina, C. B. *Clay Clay Miner.* **2000**, *48*, 424.

3. Macias, O.; Largo, J.; Pesquera, C.; Blanco, C.; González, F. *Appl. Catal. A* **2006**, *314*, 23.

4. Turhan, Y.; Dogan, M.; Alkan, M. *Ind. Eng. Chem. Res.* **2010**, *49*, 1503.

5. Liu, L.; Wei, S. L.; Lai, X. J. *J. Appl. Polym. Sci.* **2012**, *124*, 4107.

6. Shen, Y. H. *Chemosphere* **2001**, *44*, 989.

7. Chen, K.; Wilike, C. A.; Vyazovkin, S. *J. Phys. Chem. B* **2007**, *111*, 12685.

8. Wurm, A.; Ismail, M.; Kretzschmar, B.; Pospiech, D.; Schick, C. *Macromolecules* **2010**, *43*, 1480.

9. Ray, V. V.; Banthia, A. K.; Schick, C. *Polymer* **2007**, *48*, 2404.

10. Xi, Y. F.; Ding, Z.; He, H. P.; Frost, R. L. *J. Colloid. Interface Sci.* **2004**, *277*, 116.

11. Mazo, M. A.; Gusarova, E. B.; Shamaev, M. Y.; Berlin, A. A.; Balabaev, N. K.; Rutledge, G. C. *J. Phys. Chem. B* **2008**, *112*, 3597.

12. Peter, A. M.; Jennifer, L. S.; David, J.; Patrick, H. G.; Richard, A. V. *J. Phys. Chen. B* **2008**, *112*, 10544.

13. Du, X. H.; Yu, H. O.; Wang, Z.; Tang, T. *Polym. Degrad. Stab.* **2010**, *95*, 587.

14. Abdallah, W.; Yilmazer, U. *Thermochim. Acta* **2011**, *525*, 129.

15. Zang, Y. L.; Xu, W. J.; Qiu, D. Y.; Chen, D.; Chen, R. Y.; Su, S. P. *Thermochim. Acta* **2008**, *474*, 1.

16. Xie, W.; Gao, Z. M.; Pan, W. P.; Hunter, D.; Singh, A.; Vaia, R. *Chem. Mater.* **2001**, *13*, 2979.

17. Patel, H. A.; Somani, R. S.; Bajaj, H. C.; Jasra, R. V. *Appl. Clay Sci.* **2007**, *35*, 194.

18. Wang, Z.; Du, X. H.; Song, R. J.; Meng, X. Y.; Jiang, Z. W.; Tang, T. *Polymer* **2007**, *48*, 7301.

19. Sanchez-Martin, M. J.; Dorado, M. C.; Hoyo, C. D.; Rodriguez-Cruz, M. S. *J. Hazard. Mater.* **2008**, *150*, 115.

20. Onder, E.; Sarier, N.; Ukuser, G.; Ozturk, M.; Arat, R. *Thermochim. Acta* **2013**, *566*, 24.

21. Sarier, N.; Onder, E.; Ersoy, S. *Colloids Surf. A* **2010**, *371*, 40.

22. Liang, C. G.; Wang, X. M. *Ind. Miner. Proc.* **2009**, *4*, 8.

23. Chen, H. Q.; Li, Y. Y.; Zhu, J. W.; Yang, X. J.; Liu, L. D.; Wang, X. *Chin. J. Inorg. Chem.* **2004**, *20*, 251.

24. Feng, L. T.; Zhang, B. Y.; He, X. J. *J. Appl. Polym. Sci.* **2009**, *112*, 971.

25. Gong, F. L.; Feng, M.; Zhao, C. G.; Zhang, S. M.; Yang, M. S. *Polym. Degrad. Stab.* **2004**, *84*, 289.

26. Guo, Y.; Zheng, Y. Y.; Qiu, S. C.; Zeng, A. R.; Li, B. M. *J. Rare Earth* **2011**, *29*, 401.

27. Zheng, Y. Y.; Cai, W. L.; Fu, M. L.; Wang, C. Y.; Zhang, X. *J. Rare Earth* **2005**, *23*, 172.

28. Fang, L.; Song, Y. H.; Zhu, X. N.; Zheng, Q. *Polym. Degrad. Stab.* **2009**, *94*, 845.

29. Zhu, X. N.; Song, Y. H.; Chen, S. H.; Du, P. H.; Zheng, Q. *Polym. Int.* **2011**, *60*, 1355.

30. Fan, X. W.; Chen, G.; Wan, S. K.; Su, Q. D. *Spectrosc Spect. Anal.* **1999**, *19*, 772.

31. Peng, Z. B.; Hu, B.; Su, Q. D.; Qu, J. Z. *J. Rare Earth* **2003**, *21*, 328.

32. Zheng, Y. Y.; Cai, W. L.; Fu, M. L.; Sun, R. Q. *Spectrosc Spect. Anal.* **2004**, *24*, 1533.

33. Wan, C. Y.; Qiao, X. Y.; Zhang, Y.; Zhang, Y. X. *Polym. Test.* **2003**, *22*, 453.

34. Sterky, K.; Hjertberg, T.; Jacobsen, H. *Polym. Degrad. Stab.* **2009**, *94*, 1564.